Measurement of the upper critical magnetic field of superconductors with magnetic impurities

Thomas R. Lemberger* and D. M. Ginsberg
Department of Physics and Materials Research Laboratory, University of Illinois at Urbana-Champaign, Urbana, Illinois 61801
(Received 5 June 1978)

We have measured the upper critical magnetic field, $H_{c2}(T)$, for In-Mn and Pb-Mn films, in which the Mn is a magnetic impurity. The results are compared with the additive-pair-breaking theory of Fulde and Maki, which predicts that the pair-breaking effect of the magnetic impurities is temperature-independent and that the pair-breaking effects of the magnetic impurities and of the applied magnetic field are additive. Furthermore, the theory predicts the explicit temperature dependence of $H_{c2}(T)$. The results indicate that the temperature dependence of H_{c2} is well described by the Fulde-Maki theory for In-Mn, but not for Pb-Mn, probably because of the strong-electron-phonon coupling in Pb. For both In-Mn and Pb-Mn, the results indicate that the pair-breaking effect of the magnetic impurities is temperature independent, and that the pair-breaking effects of the magnetic impurities and the applied magnetic field are additive, so the concepts inherent in the Fulde-Maki theory are supported. We find no evidence in the data of the Kondo effect or of impurity spin alignment.

I. INTRODUCTION

A. Background

It was discovered in the 1950s that small concentrations of magnetic impurities severely depress the superconducting transition temperature of the host metal.[1,2] The fact that the strength of the depression was correlated with the spin of the impurity, and not with its magnetic moment, led Herring[3] to suggest that the interaction responsible for the effect of the magnetic impurities was the exchange interaction between the impurity spins and the conduction electrons. Abrikosov and Gor'kov (AG)[4] showed how to incorporate this interaction into calculations of superconducting properties. The theory was later developed by Skalski *et al.*[5] and by others.[6] Experimental studies of the tunneling characteristics of Pb-Gd by Woolf and Reif,[7] of the specific-heat jump in La-Gd by Finnemore *et al.*,[8] and other studies[9] verified the basic correctness of the AG theory. However, it was found that the AG theory was not successful for magnetic impurities from the 3*d* elements. This was shown in measurements of tunneling into In-Fe and Pb-Mn alloys,[7] of far-infrared absorption in Pb-Mn alloys,[10] and of the thermal conductivity of In-Mn, Pb-Mn, and In-Cr alloys.[11] The source of the disagreement was thought to be that AG had treated the exchange interaction as a weak interaction; they calculated its effect in the first Born approximation.

An attempt to treat the exchange interaction to higher order was made by Shiba,[12] (and later, but independently, by Rusinov[13]). In fact, by treating the impurity spins as though they were classical spins, he was able to treat the impurities exactly. Calculations based on this theory agreed with the tunneling data on Pb-Mn,[14,15] but not with the tunneling data on In-Fe.[16] Other disagreement between theory and experiment was discussed by Ginsberg.[17]

Müller-Hartmann and Zittartz (M-HZ)[18] constructed a theory in which they included the quantum-mechanical nature of the impurity spins. This theory was later extended by Schuh and Müller-Hartmann.[19] These theories reduced to the AG theory in the limit of zero Kondo temperature. The agreement of the M-HZ theory with experiment has recently been reviewed by Takayanagi and Sugawara.[20]

A calculation of H_{c2} based on the AG theory was performed by Fulde and Maki (FM),[21] and a calculation of H_{c2} based on the M-HZ theory was first performed by Maki[22] and was later improved by Schuh and Müller-Hartmann.[19] These calculations showed that the Kondo effect could cause the temperature dependence of H_{c2} to deviate sharply from the prediction of the FM theory if the Kondo temperature is near the superconducting transition temperature of the host.

These theories all assumed that the impurity spins are randomly distributed and oriented. However, calculations have been made of properties of superconductors assuming some order among the impurity spins. In particular, Fischer[23] calculated the effect on H_{c2} of paramagnetic impurity spin alignment caused by the applied field. Benemann[24] calculated some of the effects of impurity alignment due to impurity-impurity interactions. (Since these impurity-impurity interactions typically become important only when the impurity concentration is high enough to reduce the transition temperature of the alloy to below half of the transition temperature of the pure host,[25] we avoided them in our experiment by keeping the

impurity concentration lower than that amount.)

These theories are discussed in more detail in Sec. I B. Even if they are not exact, they provide at least a qualitative idea of how the temperature dependence of H_{c2} might be affected by magnetic impurities. These qualitative effects may be independent of some of the approximations of the theories, e.g., weak electron-phonon coupling. Therefore, even without an exact theory, it may be possible to interpret the data by using these qualitative results.

B. Theory

This section describes the theories of magnetic impurities in superconductors due to Abrikosov and Gor'kov (AG) and to Shiba, and the predictions of these theories for the temperature dependence of the upper critical magnetic field H_{c2}.

AG assumed that the impurity spins have an infinite lifetime and that they interact weakly with the conduction electrons through the exchange interaction

$$H_{ex} = -2J\vec{S}\cdot\vec{s}_e \ , \tag{1}$$

where J is the exchange constant, $\vec{S}$ is the impurity spin, and $\vec{s}_e$ is the conduction-electron spin. They obtained an expression for the dependence of the transition temperature of a superconductor with magnetic impurities:

$$\ln(T_c/T_{c0}) = \psi(\tfrac{1}{2}) - \psi(\tfrac{1}{2} + \alpha_i/2\pi T_c) . \tag{2}$$

Here, T_c is the transition temperature of the alloy, T_{c0} is that of the host, ψ is the digamma function, units are used in which Boltzmann's constant is equal to 1, and α_i is the spin-flip scattering rate from the magnetic impurities, given by

$$\alpha_i \equiv 1/\tau_s = \tfrac{1}{2} n_i \pi N(0) J^2 S(S+1) , \tag{3}$$

where n_i is the concentration of the magnetic impurities and $N(0)$ is the density of electronic states at the Fermi energy for one spin direction. α_i is commonly referred to as a "pair-breaking" parameter, because it characterizes the strength of the pair-breaking effect of the magnetic impurities on the conduction electrons.

Shiba extended this theory by making all of the assumptions of the AG theory and assuming that the impurity spins are classical rather than quantum mechanical. He was then able to treat the exchange interaction exactly. This theory necessarily reduces to the AG theory in the limit of weak exchange coupling. In Shiba's theory, the dependence of T_c on the magnetic impurity concentration is the same as in the AG theory as given in Eq. (2), except that the expression for α_i is given by a different expression:

$$\alpha_i = [n_i/2\pi N(0)](1 - \epsilon_0^2) . \tag{4}$$

ϵ_0 can be expressed in terms of other constants in the theory as

$$\epsilon_0 = \left| \frac{1 - [\frac{1}{2}\pi JSN(0)]^2}{1 + [\frac{1}{2}\pi JSN(0)]^2} \right| . \tag{5}$$

From Eq. (5), it is clear that

$$0 \leq \epsilon_0 \leq 1 ; \tag{6}$$

when ϵ_0 approaches 1, the Shiba theory reduces to the AG theory. Equation (2) can be written in the form

$$\ln(T_c/T_{c0}) = \psi(\tfrac{1}{2}) - \psi[\tfrac{1}{2} + 0.140\,(n_i/n_{cr})(T_{c0}/T_c)] , \tag{7}$$

where n_{cr} is the concentration of magnetic impurities required to reduce T_c/T_{c0} to zero.

Fulde and Maki calculated $H_{c2}(T)$ by using the AG theory. They showed that in dirty, three-dimensional, type-II superconductors, the pair-breaking effects of the field and of the impurities are additive, i.e.,

$$\ln(T/T_{c0}) = \psi(\tfrac{1}{2}) - \psi[\tfrac{1}{2} + \alpha(T)/2\pi T] , \tag{8}$$

where

$$\alpha(T) = \alpha_i + \alpha_H(T) \tag{9}$$

and

$$\alpha_H(T) = DeH_{c2}(T)/c . \tag{10}$$

Here, D is the electron diffusion constant, given by

$$D = \tfrac{1}{3} v_f l , \tag{11}$$

v_f is the Fermi velocity, and l is the electron mean free path. Dirty, three-dimensional, type-II superconductors have the properties

$$l \ll \xi_0 , \tag{12}$$

$$d \gg (l\,\xi_0)^{1/2} , \tag{13}$$

$$\kappa \geq \tfrac{1}{2} \tag{14}$$

where d is the thickness of the sample, ξ_0 is the coherence length corresponding to infinite mean free path, and κ is the Ginzburg-Landau parameter. Equation (8) has the same form as Eq. (2), but with a pair-breaking parameter which corresponds to the sum of the pair-breaking effects of the magnetic impurities and the applied magnetic field.

A calculation of H_{c2} according to the Shiba theory has not yet been carried out. Presumably such a calculation would also show the property of additive pair breaking, since the result would have to reduce to Eq. (8) in the limits both of weak exchange coupling and of zero impurity concentra-

tion. If so, the temperature dependence of H_{c2} in the Shiba theory should be the same as that calculated by FM in the AG theory. We therefore compare our results with the predictions of the FM theory, but with α_i given by Eq. (4).

In principle, Eq. (8) can be inverted to give $\alpha(T)$. Using Eqs. (9) and (10), $H_{c2}(T)$ can be found:

$$H_{c2}(T) = c\alpha(T)/De - (c/De)\alpha_i . \quad (15)$$

Equation (15) indicates that if one measured the upper critical magnetic field of a pure superconductor which had a diffusion constant D^p, one would expect to find

$$H^p_{c2}(T) = c\alpha(T)/D^p e . \quad (16)$$

If one then measured the upper critical magnetic field of the same superconductor but with magnetic impurities and with diffusion constant D, one would expect to find

$$H_{c2}(T) = \frac{D^p}{D} H^p_{c2}(T) - (c/De)\alpha_i . \quad (17)$$

Equation (17) is the central equation in the analysis of our data. It shows explicitly that even if we do not assume that the FM prediction for $\alpha(T)$ is correct, we can still test the prediction of additive pair breaking with a temperature-independent pair-breaking parameter representing the effect of the magnetic impurities. We do this by using the measured $H^p_{c2}(T)$ curve in Eq. (17). This may be important in strong-coupling superconductors, where $H_{c2}(T)$ can differ significantly from the predictions of weak-coupling theories.[26]

The work of Schuh and Müller-Hartmann[19] and of Fischer[23] indicate that the Kondo effect and impurity spin alignment with the applied field can cause large deviations from the prediction of Eq. (17).

C. Previous work

Measurements of $H_{c2}(T)$ on superconductors with rare-earth impurities showed that additive pair-breaking applies to these systems. This work was pioneered by Parks and his co-workers[27] and has been well reviewed in Refs. 9 and 28. A study of $H_{c2}(T)$ on a superconductor with a $3d$-element impurity was made by Barth *et al.*[29] on the Mo-Re-Fe system. Their results were consistent with the FM theory. However, their data were sparse, and the scatter in them was large enough that only the gross features of the theory could be tested. The scatter in our data is less than $\frac{1}{10}$ as large, and we took about twice as many data points for each sample.

Previous measurements of $H_{c2}(T)$ on quench-condensed films of pure indium[30] and pure lead[31] have been made. Our data are consistent with these, as will be discussed later.

D. Purpose of this experiment

The purpose of this experiment was to see whether the pair-breaking effects of magnetic impurities and applied magnetic fields on the superconducting state are additive with a temperature-independent pair-breaking parameter describing the effect of the magnetic impurities, as one would expect from the FM theory. We hoped to be able to identify the cause of any deviation from the FM theory from a knowledge of the expected qualitative effects of interactions which were ignored in the theory.

For these purposes, very precise measurements of $H_{c2}(T)$ were needed. Since we determined H_{c2} from the resistance of the sample films, we narrowed the width of the field region in which the transitions occurred by scribing the edges of our samples away from the middle. This method of eliminating edge effects, unlike the technique of coating the entire film with a paramagnetic metal like Fe,[31] cannot have any effect on the properties of the middle of the film. Unfortunately, this scribing required that we use an electrode geometry which did not allow a precise measurement of the sample resistivity; the absolute and relative resistivities of our samples could be determined to an accuracy of only ±40%. Therefore, we could not determine the electron diffusion constant D experimentally, and comparison of our $H_{c2}(T)$ data with the theoretical values could be made only by using D as a fitting parameter.

Indium and lead were chosen as the host superconductors because they had transition temperatures which were easily accessible, they had low evaporation temperatures,[32] and they had smoothly varying densities of states which should not have been affected much by either quench-condensing the samples or by alloying them with small amounts of manganese.

Manganese was chosen as the impurity because data on In-Mn and Pb-Mn alloys indicated that Mn supported a localized moment in these quench-condensed materials, because Mn was known to have a strong effect on the value of T_c for In,[33] and Pb,[34] and because it had a low evaporation temperature.[32] This experiment is part of a series of investigations which are being performed by our research group on these alloys.

To prevent the manganese from precipitating, the sample films had to be quench condensed at liquid-helium temperatures. They could not be warmed up until after all the data had been taken.

II. EXPERIMENTAL PROCEDURES

A. Apparatus

We used an all-metal cryostat to cool the sample. The assembly which held the substrate was attached to the bottom of a liquid-helium reservoir. It was surrounded by two concentric heat shields, the inner one at 4.2 K and the outer at 77 K. The sample and heat shields were surrounded by a vacuum jacket which was narrow enough to fit between the pole faces of an external electromagnet. The cryostat was constructed almost completely from nonmagnetic materials to avoid distortion of the applied magnetic field.

The substrates were pieces of Z-cut, optically polished, crystal quartz, which were carefully cleaned before each run. Gold electrodes for measuring the four-terminal resistance of the sample film were evaporated onto the substrates before they were inserted into the cryostat. The substrates were thermally linked to the copper substrate holder with a thin layer of N grease.

The sample films were made by evaporating pellets with the desired alloy composition upward through holes in the bottoms of the heat shields onto a cold (~4.5-K) substrate. The procedure for making the ingots from which the pellets were cut has been described by Przybysz and Ginsberg.[11] Typically, there were 50 to 100 pellets, which weighed a total of about 200 mg. These were dropped into a tungsten boat which was at a temperature of about 1100 °C. Each pellet evaporated in several seconds and added about 30 Å to the sample film's thickness. The pressure in the cryostat remained below 5×10^{-6} Torr during this procedure.

The sample film was 0.95 cm wide after it was scribed and 1.6 cm long. It overlapped the gold electrodes so that there were two electrodes on each of the unscribed edges. Because of this side-by-side electrode configuration, because the gold electrodes had about the same resistance per square as the samples, and because the edges of the samples which overlapped the electrodes had different properties from the rest of the sample, the current pattern in each sample was very uncertain. The estimated uncertainty in the relative and absolute resistivities of the samples was 40%.

After all the pellets had been evaporated, the sample film was rotated from its original horizontal position to a vertical position so that it would be parallel to the magnet's pole faces. Then, using a mechanical assembly which was attached to the substrate holder, the edges of the sample film were scribed away from the middle. The sample was kept below 4.2 K during this operation. Throughout the entire experiment, the sample temperature was kept below 8 K.

The temperature of the sample was determined with a germanium thermometer to a precision of 0.005% and to an estimated accuracy of 0.1%. The temperature was electronically regulated to better than 0.3 mK above 5 K and to better than 0.1 mK below 5 K. The carbon resistor which was used as the sensing element in the electronic temperature regulator was found to have only a very slight dependence on the applied magnetic field; when the magnetic field was increased from 0 to 4 kG, its resistance changed by an amount equivalent to a change in temperature of 0.7 and 0.4 mK at temperatures of 2 and 3.6 K, respectively.

The magnetic field was generated by an electromagnet which could achieve fields of up to 4 kG with the 4-in. pole gap which we used. The magnet generated a field which was rated to be stable to 0.1% against line voltage changes or load resistance changes of 10%. The maximum ripple in the field was supposed to be less than 0.01% of the field value. The field was supposed to be homogeneous to 1% in a 1-in.-diam sphere centered between the pole faces. The magnet was mounted on a cart which moved on tracks so that it could be moved up to and away from the cryostat.

The magnetic field was measured with a bismuth-film Hall probe which was located next to the sample. To increase the sensitivity of the Hall probe while keeping power dissipation down, the Hall probe was operated at a frequency of 1 kHz and a lock-in amplifier was used to detect the transverse voltage across the probe. The Hall probe was calibrated against a rotating-coil gaussmeter in each run before any H_{c2} data were taken. The calibration was checked after all the data were taken. The calibration was found to be slightly temperature dependent for temperatures above 4.5 K and for fields above 2 kG. Hence, during the Pb-Mn runs, the probe was calibrated at several temperatures, and the field value associated with a particular Hall voltage at a particular temperature was interpolated by using this calibration. We estimate that the accuracy of the calibration was about 2 G.

B. Data-taking procedures

After a sample film had been successfully deposited, rotated, and scribed, its zero-field resistive transition was measured. This was done by using the electronic temperature regulator to step the sample temperature through the transition. At appropriate temperature intervals, the sample resistance and the temperature of the germanium thermometer were measured. The Hall probe was then calibrated, as described in

Sec. II A. At this point, resistive transitions of the sample film were measured as a function of field strength at several different temperatures. This was done analogously with the zero-field transitions. First, the temperature was measured with the germanium thermometer. Then, with the electronic temperature regulator holding the temperature constant, the field was turned on and slowly stepped through the transition. At appropriate field intervals, the sample resistance and the Hall voltage were measured.

During the In-Mn runs, when the field was above the transition field of most of the film, the sample temperature was raised to about 1 K above the zero-field transition temperature and then allowed to cool back to the original temperature. Then the transition in a decreasing field was measured. This was an attempt to see if there was any hysteresis in the transitions. None was ever found.

For the Pb-Mn data, which were taken after the In-Mn data, another step was added. After the discrete data points had been taken, the resistance of the sample film and the output from the Hall probe were put into the X and Y axes of an X-Y chart recorder, and a continuous trace of the resistive transition was obtained by slowly increasing the strength of the magnetic field through the transition. This continuous curve was combined with the discrete data to provide a complete description of the shape and position of the transition.

When a sufficient number of finite-field transitions had been measured, the Hall-probe calibration was checked. Then the cryostat was allowed to slowly warm up to room temperature. The sample film was removed from the cryostat and covered with a thin (~1000-Å) layer of silver so that its thickness could be measured with an interferometric method due to Tolansky.[35] Detailed descriptions of the apparatus and procedures used to calibrate the Hall probe and thermometer, clean the substrate, etc. are in Ref. 36.

III. RESULTS AND DISCUSSION

A. Resistive transitions

In this section, we discuss the shapes of the zero-field and finite-field resistive transitions and how these transitions are used to determine $H_{c2}(T)$. The measuring currents used to obtain these curves ranged from 40 to 100 μA.

Figures 1 and 2 show zero-field transitions of pure In and pure Pb films, both before and after the films were scribed. Changes caused by the scribing are evident. The sharpness of the transitions of all of the scribed samples indicates that the samples were homogeneous. The widths of

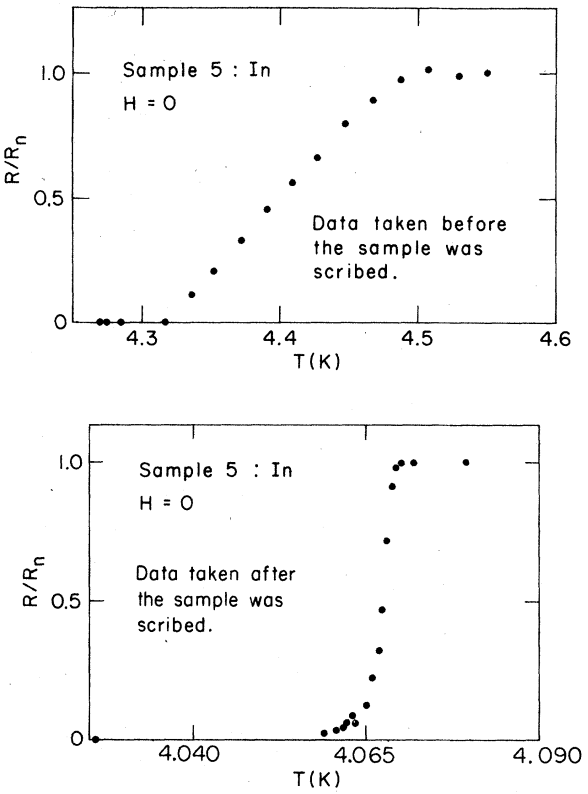

FIG. 1. Zero-field resistive transition of sample 5. R is the sample resistance, and R_n is its normal-state value. The transition is shown both before and after the sample was scribed.

the zero-field transitions of all of our samples are listed in Table I.

Figure 3 shows a typical finite-field transition for an In-Mn sample. The transition shows three distinct regions: a foot, a linear region, and a

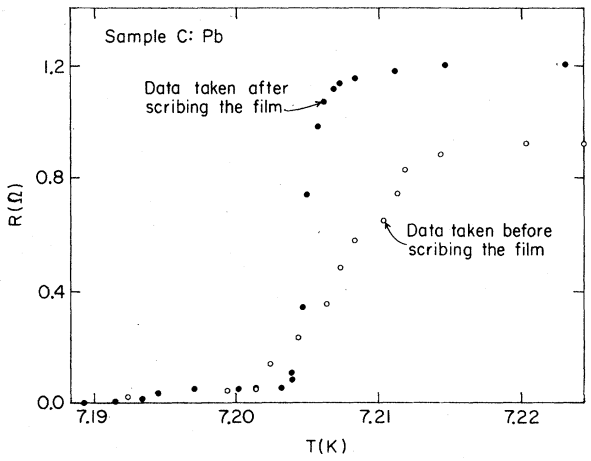

FIG. 2. Zero-field resistive transition of sample C. R is the sample resistance. The transition is shown both before and after the sample was scribed.

TABLE I. Sample film characteristics. d is the film thickness; T_c is the transition temperature, determined by extrapolating the steep, linear part of the resistive transition curve to the normal-state resistance; ΔT_c is the 10%–90% transition width. The values given for T_c are on the NBS-65 scale.

Sample	Host	at. % Mn ±5%	d (Å) ±2%	T_c (K)	ΔT_c (mK)
5	In	0	1880	4.069	3
7	In	0	1410	4.173	4
13	In	0.030	1930	2.746	10
19	In	0.039	2546	2.227	38
C	Pb	0	1650	7.206	3
H	Pb	0	1815	7.205	2
D	Pb	0.057	1800	6.339	3
E	Pb	0.128	1500	4.805	6
F	Pb	0.160	1470	4.494	6
G	Pb	0.200	1210	3.711	5

gradual approach to the normal-state resistance. For the In-Mn samples, the foot is unaffected by doubling or halving the measuring current, but the other two regions are affected slightly. This current dependence could be due to Joule heating and/or to a residual filamentary superconducting structure. We assign $H_{c2}(T)$ to three different points on the transition to see if the results depend on which point is chosen. Hence, there are three data sets for each sample; Fig. 3 indicates the correspondence between the point and the data set. We estimate that the uncertainty in determining the three points from the transition curves is about ±1 G. We do not use the point where the sample resistance first becomes nonzero because it is too poorly defined.

Figure 4 shows a typical finite-field transition for a Pb-Mn sample. The transition shows three distinct regions: a foot, a linear region, and a gradual approach to the normal-state resistance. These curves are unaffected by doubling or halving the measuring current. The bump in Fig. 4 is caused by the transition from superconducting to normal in the two unscribed edges of the sample. This transition changes the current pattern in the sample and hence changes the four-terminal resistance. This behavior has been verified with models of the sample geometry made with conducting paper. Again, three points on the transition were chosen as appropriate places to assign H_{c2}. Hence, there are three data sets for each sample; Fig. 4 indicates the correspondence between the point and the data set.

Work on the problem of choosing which point on the resistive transition to use has been done by Cape[37]

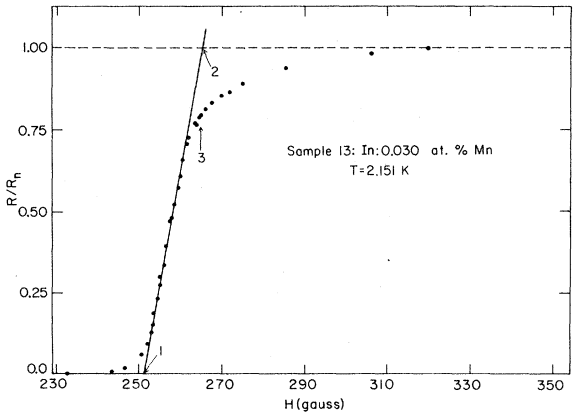

FIG. 3. Typical finite-field resistive transition of sample 13. R is the sample resistance, and R_n is its normal-state value. The points on the curve which correspond to data sets 1, 2, and 3 are indicated.

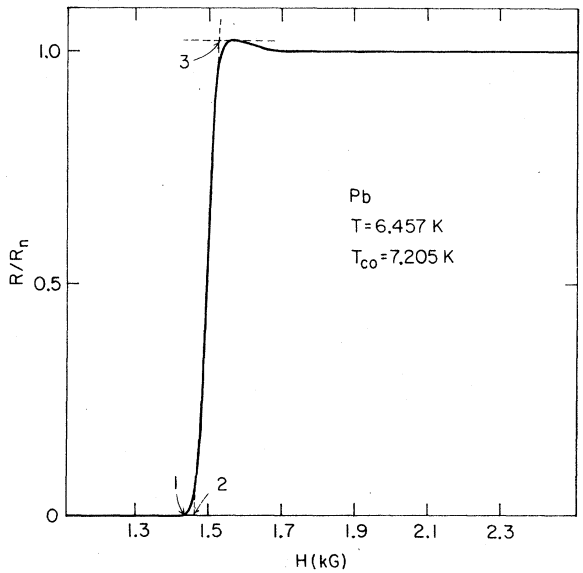

FIG. 4. Typical finite-field resistive transition of sample C. R is the sample resistance, and R_n is its normal-state value. The points on the curve which correspond to data sets 1, 2, and 3 are indicated.

and by Miller and Cody.[38] Cape worked with chromium-plated foils and found that H_{c2} corresponds to the knee in the transition. Miller and Cody worked with scribed films and found that H_{c2} corresponds to the point where the sample resistance first becomes nonzero.

B. $H_{c2}(T)$ data

1. In-Mn

Characteristics of the four In-Mn samples on which critical field measurements were made are listed in Table I. Many other samples were made on which no critical-field data were taken, either because of some mechanical failure in the cryostat or because the width of the zero-field transition was judged to be too large. These will not be discussed further.

To compare our results with the FM theory, we first determine how well the samples satisfy the criteria expressed in Eqs. 12–14. To within the uncertainty in the sample resistances discussed earlier, all four of the samples on which critical-field data were taken have the same resistivity, 10 $\mu\Omega$ cm. Using the Goodman approximation[39] to the Gor'kov[40] relation between the resistivity and κ,

$$\kappa = \kappa_0 + 7.53 \times 10^3 \, \rho \gamma^{1/2}, \tag{18}$$

where ρ is the resistivity in Ω cm and γ is the electronic-specific-heat constant in erg/cm^3 K^2, we can verify that the samples were type-II superconductors. Substituting $\rho = 10^{-5}$ Ω cm from our data, and[41] $\gamma = 1.06 \times 10^3$ erg/cm^3 K^2, and[42] $\kappa_0 = 0.062$, we find that $\kappa \approx 2.5$.

The electron mean free path l in the samples can be roughly determined from the resistivity ρ by assuming that the product ρl is a constant. It can also be estimated from the value of D found by fitting the $H_{c2}(T)$ data with the FM theory. (The fitting procedure will be described later.) Using a value[43] of 1.11×10^{-11} Ω cm^2 for ρl and, following Bergmann,[30] a value for v_f of 0.97×10^8 cm/sec, and an average value for D of 21 cm^2/sec, we find that the mean free path is either

$$l = 3D/v_f \approx 65 \text{ Å} \tag{19}$$

or

$$l = \rho l/\rho \approx 111 \text{ Å}. \tag{20}$$

Within the large uncertainties in ρ, ρl, and v_f, this agreement is good. Anderson and Ginsberg[44] have reviewed the experimental values of ρl for indium.

The coherence length ξ_0, corresponding to infinite mean free path can be estimated from the relation[45]

$$\xi_0 = \hbar v_f/\pi\Delta(0) = \hbar v_f/1.76\,\pi k_B T_{c0} \approx 3400 \text{ Å}. \tag{21}$$

We can use this value to determine that

$$l/\xi_0 \approx \tfrac{1}{40}, \tag{22}$$

and

$$d/(\xi_0 l)^{1/2} \approx 3.5. \tag{23}$$

Therefore, using Eqs. (22) and (23), we find that the samples are dirty, reasonably three-dimensional films, as the FM theory assumes.

The critical-field data and a fit to the FM theory are shown in Figs. 5–8. To fit the theory to the data, the value of the electron diffusion constant D and the transition temperatures of the alloy, T_c, and of the host, T_{c0}, are used as fitting parameters. Of course, to fit the data for the pure indium samples, T_c and T_{c0} are set equal to each other. It should be noted that the fits to the data for samples 13 and 19 are quite insensitive to the value of T_{c0} which is used. Equally good fits can be obtained with values of T_{c0} ranging from T_c to about 4.5 K. Therefore, we determine T_{c0} self-consistently for each set of data for these samples in the following manner. The values for T_{c0} and D obtained from the fits to the data for samples 5 and 7, which were pure indium, are used to estimate what value of T_{c0} corresponds to a given value of D. Then the fits to the data on samples 13 and 19 are done in such a way that the resulting values of T_{c0} and D agree with this estimate.

It is clear from Figs. 5–8 that the FM theory describes the temperature dependence of H_{c2} for all three data sets from each sample. The rms deviation of the data from the theoretical curves is about 2 G, excluding the zero-field transition point. As the figures show, the curves which fit the finite-field data do not extrapolate well to the zero-field data points in general.

The scatter in the data arises mainly from the finite precision of the sample temperature measurement, the uncertainty in determining the positions of points 1, 2, and 3 from the transition curves, and the uncertainty in the Hall-probe calibration. We estimate that the scatter in the data should be about 2 G. Systematic uncertainties in $H_{c2}(T)$ are caused by systematic deviations of the germanium thermometer calibration from the thermodynamic scale, from the inhomogeneity of the magnetic field over the sample area, and from the lack of perfect perpendicularity between the sample and the field. We estimate that the systematic uncertainty in $H_{c2}(T)$ is about 0.2%. Therefore, the error bars on the data points in Figs. 5–8 would be smaller than the dots which are used to represent the data.

The good agreement between theory and experi-

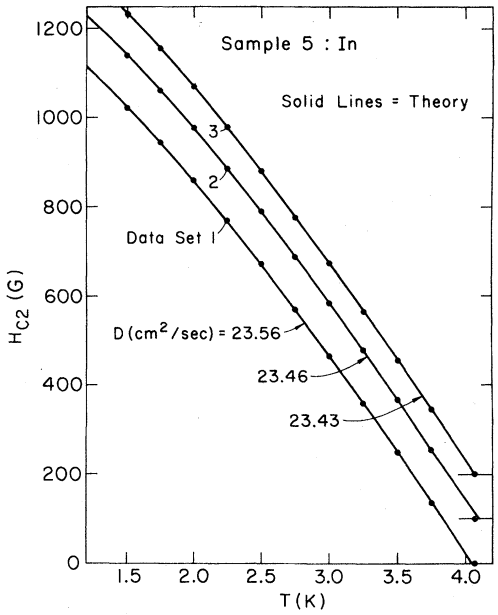

FIG. 5. Plot of the experimental values of $H_{c2}(T)$ for sample 5 compared with a fit to the FM theory. Data sets 2 and 3 are displaced upward by 100 and 200 G, respectively, for clarity.

ment is somewhat surprising because the FM theory assumes weak electron-phonon coupling and quench-condensed indium is known to be a moderately strong-coupling superconductor.[46] There is no evidence from our results for alignment of the impurity spins with each other or with the applied field. There is also no indication of the Kondo effect.

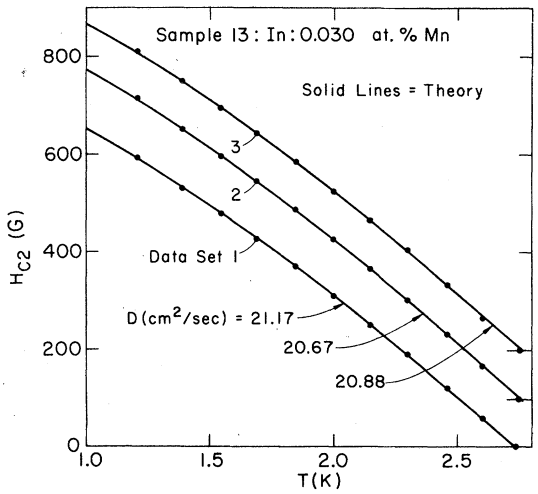

FIG. 7. Plot of the experimental values of $H_{c2}(T)$ for sample 13 compared with a fit to the FM theory. Data sets 2 and 3 are displaced upward by 100 and 200 G, respectively, for clarity.

We can compare some of our results with previous work. The chemically measured manganese concentration of the starting material, the measured transition temperature, and the estimated value of T_{c0} obtained as described above can be used together with the prediction for the dependence of T_c/T_{c0} on n_i/n_{cr}, as expressed in Eq. (7), to obtain a value for n_{cr} for samples 13 and 19. The results indicate that $n_{cr} = 0.066 \pm 0.003$ at. %

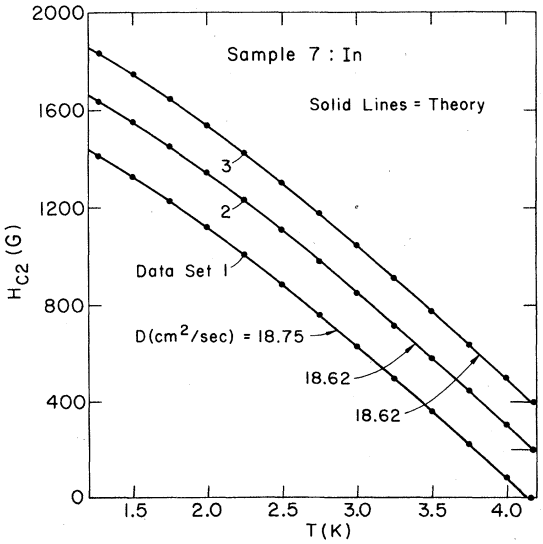

FIG. 6. Plot of the experimental values of $H_{c2}(T)$ for sample 7 compared with a fit to the FM theory. Data sets 2 and 3 are displaced upward by 200 and 400 G, respectively, for clarity.

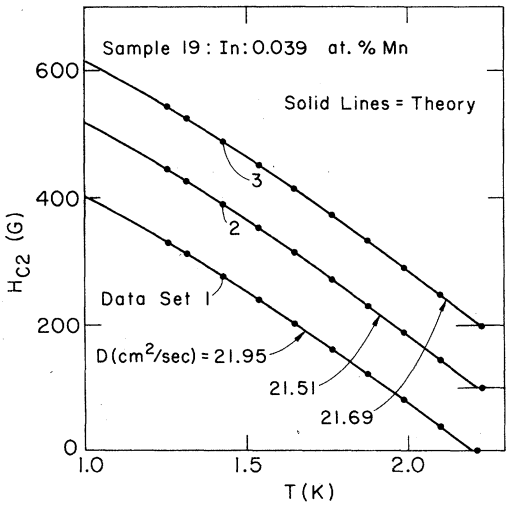

FIG. 8. Plot of the experimental values of $H_{c2}(T)$ for sample 19 compared with a fit to the FM theory. Data sets 2 and 3 are displaced upward by 100 and 200 G, respectively, for clarity.

for both samples. This value compares well with values for n_{cr} of 0.066 at.% obtained by Opitz[33] and 0.070 at.% obtained by Bjerkaas *et al.*[47]

Bergmann made quench-condensed indium films which had resistivities of about 5 $\mu\Omega$ cm and a value for $(dH_{c2}/dT)_{T_{c0}}$ of about 240 G/K. Since our films had about twice the resistivity of Bergmann's and since $(dH_{c2}/dT)_{T_{c0}}$ is proportional to the resistivity, this is good agreement. A more extensive discussion of the resistive transition curves and the $H_{c2}(T)$ data, together with tabulations of the In-Mn data, can be found in Ref. 36.

2. Pb-Mn

Table I lists characteristics of the six Pb-Mn samples on which $H_{c2}(T)$ data were taken. Two other samples were made on which no H_{c2} data were taken because of mechanical failure. These will not be discussed further. Within the uncertainty discussed above, all the Pb-Mn samples had resistivities of 22 $\mu\Omega$ cm. Using Eq. (24), a value for γ of[48] 1640 erg/cm^3 K^2, and a value for κ_0 of[31] 0.38, we find $\kappa \approx 7.1$. Using an average value for ρl of 1.4×10^{-11} Ω cm^2 (see Koepke and Bergmann[31] for a discussion of the experimental values for ρl), we estimate that $l \approx 64$ Å. ξ_0, calculated by using Eq. (21), is about 960 Å. Using these numbers, we find that

$$l/\xi_0 \approx \tfrac{1}{15}, \tag{24}$$

and

$$d/(l\xi_0)^{1/2} \approx 6. \tag{25}$$

Therefore, the samples are dirty, reasonably three-dimensional, type-II superconductors.

The temperature dependence of H_{c2} for the Pb-Mn samples, shown in Fig. 9, is qualitatively different from that predicted by Fulde and Maki. This is probably due in part to the strong electron-phonon coupling in lead.

In order to compare the theory with the data, we differentiate Eq. (17) to obtain

$$\frac{dH_{c2}}{dT} = \frac{D^{\flat}}{D}\frac{dH_{c2}^{\flat}}{dT}, \tag{26}$$

where we have assumed that $d\alpha_i/dT = 0$. Equation (26) indicates that measured values of $D\,dH_{c2}/dT$ should all lie on the same curve, regardless of the magnetic impurity concentration. dH_{c2}/dT can be determined from the data, as we describe below. Since D could not be determined accurately, it was used as a fitting parameter. Figure 10 shows that values of D can be chosen so that the $D\,dH_{c2}/dT$ curves do form a smooth curve. Within 10%, the values[36] of D which were used to obtain Fig. 10 were equal to each other.

To obtain dH_{c2}/dT from the data, we used a least-squares method to fit the data with polynomials and then differentiated the polynomials. The data for samples H, E, and G were well fitted with a single polynomial. The data for samples C, D, and F were not; hence the data were divided into two overlapping groups, and

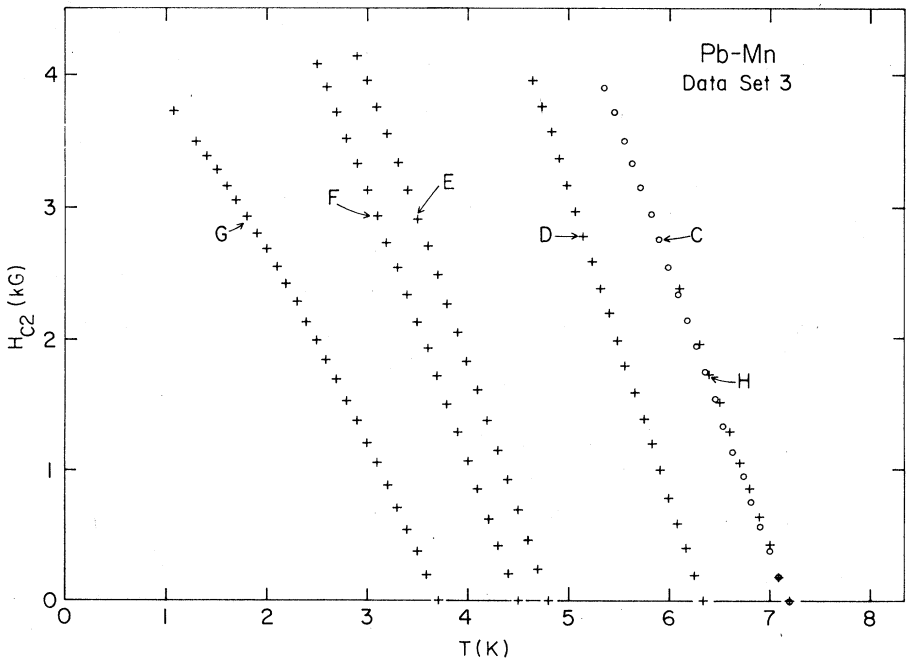

FIG. 9. Plot of the experimental values of $H_{c2}(T)$ for the Pb-Mn samples, data set 3.

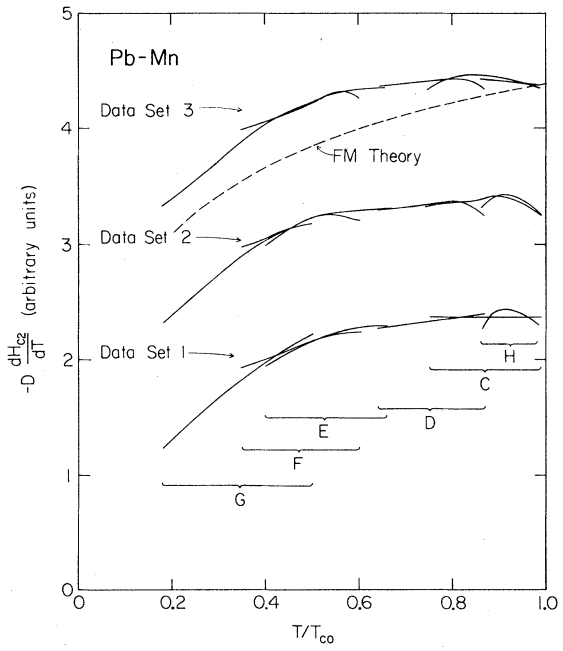

FIG. 10. Plot of $D\ dH_{c2}/dT$ for the Pb-Mn samples, where dH_{c2}/dT is determined from the $H_{c2}(T)$ data, and D is a fitting parameter chosen to give a smooth composite curve. The curves for the data sets 2 and 3 are displaced upward by 1 and 2, respectively, for clarity.

each group was fitted separately. With only one exception, the polynomials had three or fewer terms in them. The rms deviation of the data from the polynomials was about 6 G for data set 1 and 2.5 G for data sets 2 and 3; point 1 on the transition curves was quite ill-defined compared to points 2 and 3.

The sources of uncertainties in the Pb-Mn data are the same as for the In-Mn data, but some of the magnitudes are different. We estimate that the scatter in the data should be about 8, 4, and 4 G for data sets 1, 2, and 3. The systematic uncertainties in the data are the same as for the In-Mn data, 0.2%. We estimate that the uncertainty in the shapes of the $D\,dH_{c2}/dT$ curves in Fig. 10 is about 2% for data set 1 and about 1% for data sets 2 and 3.

Note that if α_i were temperature dependent, then there would be another term on the right-hand side of Eq. (26) proportional to $d\alpha_i/dT$. This term would imply that a discontinuous change in magnetic impurity concentration would cause a discontinuous change in $D\,dH_{c2}/dT$. With the method of analysis which we use, this discontinuity would not be seen because D is chosen to connect the $D\,dH_{c2}/dT$ curves together smoothly. However,

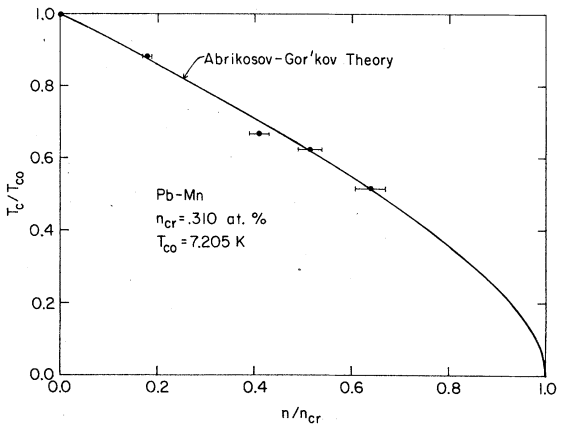

FIG. 11. Plot of T_c/T_{c0} vs n_i/n_{cr} for the Pb-Mn samples. The critical concentration n_{cr} was chosen to provide a reasonable fit to the theoretical curve.

there would still be a discontinuity in the second derivative $D\,d^2H_{c2}/dT^2$.

There is no evidence in the data for either impurity spin ordering or for the Kondo effect. There is, however, a bump in dH_{c2}/dT, which is evident in Fig. 10 in the data for pure Pb (samples C and H), for sample D and, to a lesser extent, for sample F. This bump corresponds to a region of slight positive curvature in the $H_{c2}(T)$ data. We do not understand this positive curvature. We note that it is also evident in the data of Koepke and Bergmann[31] for pure Pb.

Figure 11 shows the measured values of T_c/T_{c0} plotted vs n_i/n_{cr}, with $n_{cr}=0.310$ at.%, and compared to the AG prediction. The good agreement between the data and the theory indicates that there are probably no impurity-impurity interactions in the samples.[24] The value for n_{cr} of 0.310 at.% does not agree well with Barth's[34] value of 0.236 at.%.

Koepke and Bergmann found that their quench-condensed pure lead films had resistivities of about 18 $\mu\Omega$ cm and a value for dH_{c2}/dT of about 2.9 kG/K. Our pure lead films had resistivities of about 22 $\mu\Omega$ cm and a value for dH_{c2}/dT of about 2.2 kG/K. This agreement is moderately good. A more extensive discussion of the results on Pb-Mn, together with tabulations of the data, can be found in Ref. 36.

IV. CONCLUSION

We have measured the upper critical magnetic field of quench-condensed films of In-Mn and Pb-Mn. These films were dirty, reasonably three-dimensional, type-II superconductors. The edge effects common in a resistive measurement of H_{c2} were eliminated by scribing away the edges of the films.

The critical-field data on pure indium and pure lead are consistent with the results of Bergmann and of Koepke and Bergmann.

The pair-breaking effect of the magnetic impurities appears to be temperature-independent and additive with the pair-breaking effect of the applied magnetic field for both In-Mn and Pb-Mn. These results support the FM theory.

The explicit temperature dependence of H_{c2} for the In-Mn samples is the same as that expected from the FM theory, whereas that for the Pb-Mn samples is not, probably because of strong electron-phonon coupling.

There is a region of slight positive curvature near T_c in the $H_{c2}(T)$ data for Pb-Mn. The cause of this positive curvature is not known.

ACKNOWLEDGMENTS

The authors would like to thank John X. Przybysz for making some of the alloy ingots and Brian C. Gibson for writing the computer program which was used to fit polynomials to the Pb-Mn data. This research was supported in part by the NSF under Grant No. DMR 76-80159 and by the Department of Energy under Grant No. EY-76-C-02-1198. Paper based in part on the Ph.D. thesis of Thomas R. Lemberger, University of Illinois, 1978, unpublished.

*Present address: Dept. of Physics, Univ. of California, Berkeley, CA 94720.

[1]W. Buckel and R. Hilsch, Z. Phys. 128, 324 (1950).
[2]B. T. Matthias, H. Suhl, and E. Corenzwit, Phys. Rev. Lett. 1, 92 (1958).
[3]C. Herring, Physica (Utr.) 24, S184 (1958).
[4]A. A. Abrikosov and L. P. Gor'kov, Zh. Eksp. Teor. Fiz. 39, 1781 (1960) [Sov. Phys. JETP 12, 1243 (1961)].
[5]S. Skalski, O. Betbeder-Matibet, and P. R. Weiss, Phys. Rev. 136, A1500 (1964).
[6]A review of the development of the AG theory is given by K. Maki, in *Superconductivity*, edited by R. D. Parks (Marcel Dekker, New York, 1969), p. 1035.
[7]M. A. Woolf and F. Reif, Phys. Rev. 137, A557 (1965).
[8]D. K. Finnemore, D. L. Johnson, J. E. Ostenson, F. H. Spedding, and B. D. Beaudry, Phys. Rev. 137, A550 (1965).
[9]R. D. Parks, in *Superconductivity*, edited by P. R. Wallace (Gordon and Breach, New York, 1969), Vol. II, p. 625.
[10]G. J. Dick and F. Reif, Phys. Rev. 181, 774 (1969).
[11]J. X. Przybysz and D. M. Ginsberg, Phys. Rev. B 14, 1039 (1976); 15, 2835 (1977).
[12]H. Shiba, Prog. Theor. Phys. 40, 435 (1968).
[13]A. I. Rusinov, Zh. Eksp. Teor. Fiz. 56, 2047 (1969) [Sov. Phys. JETP 29, 1101 (1969)].
[14]A. N. Chaba and A. D. S. Nagi, Nuovo Cimento Lett. 4, 794 (1972).
[15]A. N. Chaba and A. D. S. Nagi, Can. J. Phys. 50, 1736 (1972).
[16]D. M. Ginsberg, Phys. Rev. B 13, 2895 (1976).
[17]D. M. Ginsberg, Phys. Rev. B 10, 4044 (1974).
[18]E. Müller-Hartmann, in *Magnetism*, edited by H. Suhl (Academic, New York, 1973), Vol. V, p. 353.
[19]B. Schuh and E. Müller-Hartmann, Z. Phys. B 29, 39 (1978).
[20]S. Takayanagi and T. Sugawara, J. Phys. Soc. Jpn. 38, 718 (1975).
[21]P. Fulde and K. Maki, Phys. Rev. 141, 275 (1966).
[22]K. Maki, J. Low Temp. Phys. 6, 505 (1972).
[23]O. Fischer and M. Peter, in Ref. 18, p. 327.
[24]K. H. Bennemann, in Ref. 9, Vol. I, p. 3.
[25]D. M. Ginsberg, Phys. Rev. B 15, 1315 (1977).
[26]D. Rainer and G. Bergmann, J. Low Temp. Phys. 14, 501 (1974).
[27]R. P. Guertin *et al.*, Phys. Rev. Lett. 20, 387 (1968).
[28]M. B. Maple, in Ref. 18, Vol. V, p. 289.
[29]N. Barth, H. E. Hoening, and P. Fulde, Solid State Commun. 5, 459 (1967).
[30]G. Bergmann, Z. Phys. 267, 287 (1974).
[31]R. Koepke and G. Bergmann, Z. Phys. 242, 31 (1971).
[32]L. Holland, *Vacuum Deposition of Thin Films* (Wiley, New York, 1958), p. 111.
[33]W. Opitz, Z. Phys. 141, 263 (1955).
[34]N. Barth, Z. Phys. 148, 646 (1957).
[35]S. Tolansky, *Multiple-Beam Interferometry of Surfaces and Films* (Oxford University, London and New York, 1948).
[36]T. R. Lemberger, Ph.D. thesis (University of Illinois, Urbana, 1978) (unpublished).
[37]J. A. Cape, Phys. Rev. 166, 432 (1968).
[38]R. E. Miller and G. D. Cody, Phys. Rev. 173, 494 (1968).
[39]B. B. Goodman, IBM J. Res. Dev. 6, 63 (1962).
[40]L. P. Gor'kov, Zh. Eksp. Teor. Fiz. 37, 1407 (1959) [Sov. Phys. JETP 10, 998 (1960)].
[41]D. K. Finnemore and D. E. Mapother, Phys. Rev. 140, A507 (1965).
[42]J. Feder and D. S. McLachlan, Phys. Rev. 177, 763 (1969).
[43]K. R. Lyall and J. F. Cochran, Phys. Rev. 159, 517 (1967).
[44]R. A. Anderson and D. M. Ginsberg, Phys. Rev. B 5, 4421 (1972).
[45]J. Bardeen, L. N. Cooper, and J. R. Schrieffer, Phys. Rev. 108, 1175 (1957).
[46]G. Bergmann, Z. Phys. 228, 25 (1969).
[47]A. W. Bjerkaas, D. M. Ginsberg, and B. J. Mrstik, Phys. Rev. B 5, 854 (1972).
[48]*American Institute of Physics Handbook*, 3rd ed., edited by D. E. Gray (McGraw-Hill, New York, 1972).